Apparent airborne sound insulation of hybrid wood-concrete masonry assemblies

Zeitler, Berndt; Sabourin, Ivan; Hoeller, Christoph; Mahn, Jeffrey; Schoenwald, Stefan

EuroNoise proceedings, 2015

Apparent Airborne Sound Insulation of Hybrid Wood-Concrete Masonry Assemblies

Berndt Zeitler, Jeffrey Mahn, Ivan Sabourin, Christoph Höller
National Research Council Canada, 1200 Montreal Road, Ottawa, Ontario, K1A 0R6, Canada

Stefan Schoenwald
Empa, Swiss Federal Laboratory for Material Science & Technology, Dübendorf, Switzerland.

Summary
As part of a research project to develop design solutions for concrete-masonry buildings for the Canadian market, the apparent sound insulation performance of hybrid assemblies with concrete masonry walls and wood joist floors was evaluated. In this paper, the effect of junction coupling is investigated in an ISO 15712 flanking prediction context. Airborne flanking path data predicted according to ISO 15712 are compared to data measured using the indirect ISO 10848 shielding method. Recommendations are made on how appropriate the application of ISO 15712 is for this type of hybrid assembly.

PACS no. 43.55.Rg

1. Introduction

The proposed revisions to the sound insulation requirements of the National Building Code of Canada (NBCC) will change the focus of the requirements from the separating wall between rooms to the system performance. To meet the proposed requirements, industry has funded research with the goal of developing design solutions for various types of constructions and materials. One of the constructions evaluated for the research combined concrete masonry walls with wood joist floors. The focus of this paper will be on two rooms built using this construction and specifically on the transmission path between the floor of the room above and the wall of the room below (see Figure 1). The measurement of the *in-situ* flanking sound reduction index using shielding will be presented as will the prediction of the value using the method of ISO 15712 [1].

The prediction model for the flanking sound reduction index according to ISO 15712-1 is defined as

$$R_{ij} = \frac{R_{i,situ} + R_{j,situ}}{2} + \overline{D_{v,ij,situ}} + 10 \log \frac{S_s}{\sqrt{S_i S_j}}. \quad (1)$$

For the case of the vertical floor-wall path, $R_{i,situ}$ and $R_{j,situ}$ are the in-situ sound reduction indexes of the floor and wall, respectively, $\overline{D_{v,ij,situ}}$ is the direction-averaged junction velocity level difference between the elements (floor and wall), and S_s, S_i, and S_j are the area of the separating element, floor and wall, respectively.

This study differs in scope from a previous study [5] conducted on the same reference specimen. While the previous study focused on the validity of predicting the normalized impact sound pressure levels using the empirical formulas of ISO 15712 to predict the velocity level difference, the current study focuses on in-situ measurements rather than on empirical predictions.

2. Specimen

A cross-section of the reference specimen (a) is shown in Figure 1. The numbers with the square borders identify the four elements, with 1 and 3 being the lower and upper walls, and 2 and 4 being the right and left floors. The construction is typical of row houses built with masonry separating walls in Canada. The separating wall was constructed of hollow core concrete blocks with a mass per unit area of $m_1(a) = m_3(a) = 227 kg/m^2$. Wood headers (38 mm x 235 mm) were attached using 16 mm threaded rods inserted through the wall. Floor joists (38 mm x 235 mm) were attached to the headers using joist hangers. The subfloor was 16 mm oriented strand board (OSB) and the ceiling was one layer of 13 mm gypsum board which was directly attached to the floor joists. In Canada, the floor-ceiling cavity may or may not include insulation. In this case, the floor-ceiling cavities were filled with 150 mm of fibrous insulation. The mass per unit area of the floors was $m_2(a) = m_4(a) = 35\, kg/m^2$.

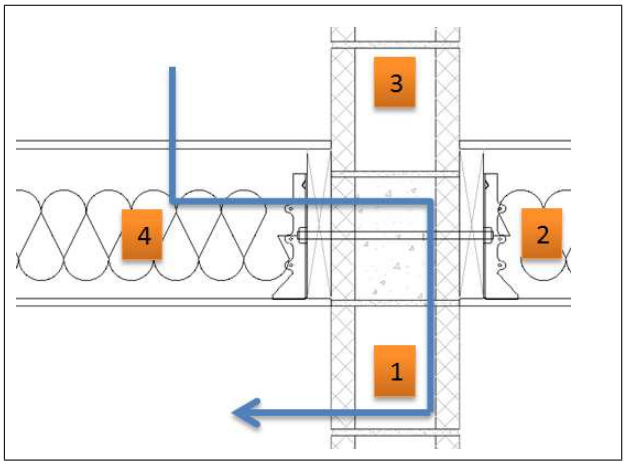

Figure 1. Cross-section of the reference specimen comprised of concrete masonry wall connected to a wood joist floor by a cross-junction. The numbering of the elements is shown. The blue arrow shows the flanking transmission path of interest (R_{41}).

Two different specimen were included in this study. The difference between the second specimen (b) and the reference specimen (a) is that the second represents apartment style construction, which has different ceiling details to suppress sound from rooms one-above-another. Instead of one layer of directly attached 13 mm gypsum board on the ceiling, two layers of 16 mm gypsum board are attached with 13 mm deep resilient metal channels spaced at 610 mm on centers. The concrete masonry wall is unchanged with $m_1(b) = m_1(a)$, however the mass of the floor elements increases to $m_2(b) = m_4(b) = 48\,kg/m^2$, due to the extra gypsum board.

3. NRC Flanking Sound Transmission Facility

NRC's Four-Room Flanking Sound Transmission Facility used in this study has one floor/wall cross-junction between the four rooms. Figure 2 illustrates the facility configuration. The permanent surfaces of the facility (top ceiling, end walls, foundation floor, and back wall) are constructed of heavy materials and are resiliently isolated from each other and from structural support members, with vibration breaks in the permanent surfaces where the specimens are installed. There is also an experimental corridor wall (sidewall) covering the front face of the facility.

The rooms have slightly different dimensions to reduce modal coupling in the low frequency range. The path of interest runs from the floor of room A to the wall of room C. The surface of the floor is $S_4 = 18.0\,m^2$ and the surface of the wall is $S_1 = 9.2\,m^2$.

The facility is equipped with an automated measurement system for data acquisition and post processing. The airborne sound reduction index is measured in both directions between the room pairs and

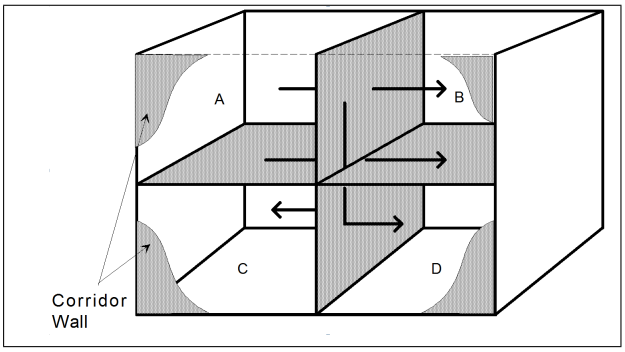

Figure 2. NRC Construction's Four-Room Flanking Sound Transmission Facility with room labels. Arbitrary sound transmission paths are displayed.

the results are averaged to reduce the measurement uncertainty due to microphone calibration errors.

4. Measurement Setup and Measurement Results

Measurements were made of all quantities in Equation 1. The equation is repeated again below with the "i"s and "j"s renamed to match the element numbering of the floor (4) and lower wall (1):

$$R_{41} = \frac{R_{4,situ} + R_{1,situ}}{2} + \overline{D_{v,41}} + 10\log\frac{S_s}{\sqrt{S_4 S_1}} \quad (2)$$

where the last term is the surface correction constant. $\overline{D_{v,41,situ}}$ was replaced by the measured direction averaged velocity level difference, $\overline{D_{v,41}}$, because the predictions and measurements are being made on the same specimen. Hence, no absorption length corrections are necessary.

Note that this measured prediction case is only used for comparison and analysis purposes. If the full specimen were built, the path data could simply be measured instead of predicted.

4.1. R_{41}, Floor-Wall Path In-situ

The flanking sound reduction index R_{41} was measured in the flanking facility according to the indirect method of ISO 10848-3 [3] for both specimens (a) and (b). Shielding was applied according to ISO 10848-1 to ensure that only the path of interest was being measured. More information about shielding approaches can be obtained in [4] and [5].

In a previous study [6] it was shown that if the junction is symmetrical and both sides of the wall are lined in the same way, the vertical floor-wall path (room A to C) is the same as the diagonal floor-wall path (room A to D). This is because velocity as well as sound radiation will be the same on both surfaces of the block wall. The reason this is important is that it is not practical to shield the floor or ceiling in order to obtain the path of interest. The path data has to be

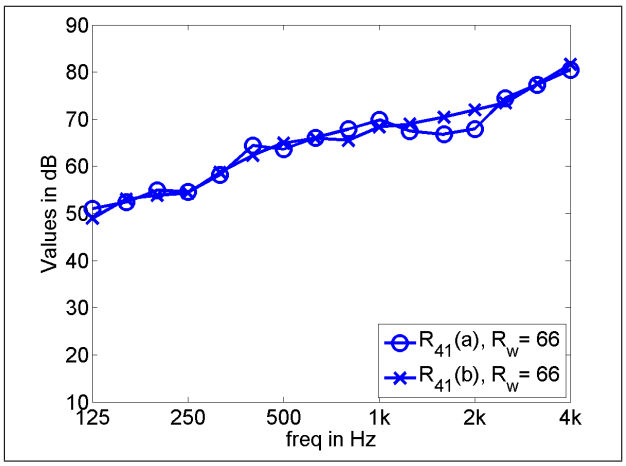

Figure 3. Flanking sound reduction index R_{41} of the path of interest for specimens (a)-o's and (b)-x's measured according to indirect method of ISO-10848-3.

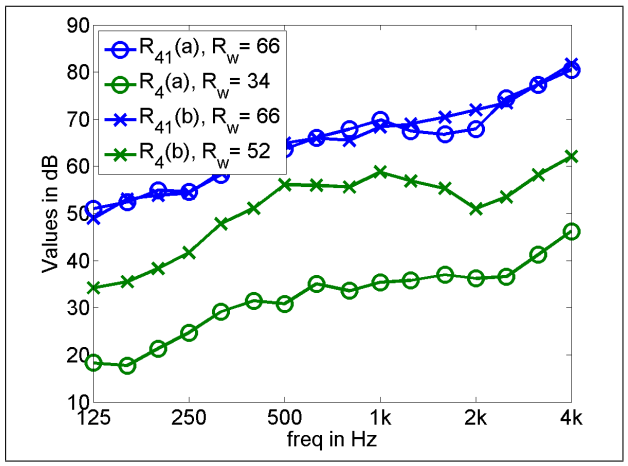

Figure 4. Direct sound reduction index R_4 through the floor for specimens (a)-o's and (b)-x's measured according to the indirect method of ISO-10848. R_{41} is also shown as a reference.

calculated from a set of measurements, each containing a different set of paths. Thus is like solving a linear equation system with several unknowns (paths) and several equations (measurements). Making this case even more difficult is the fact that the direct floor-ceiling path is clearly dominant and the visibility of the path of interest is very small. Thus the repeatability error could be larger than the influence of the path of interest. Hence measurements were made from room A to D. As the upper walls were shielded, only two diagonal paths exist (floor-ceiling and floor-wall path), and only two shielding conditions are necessary to solve for the two paths.

The measured values of R_{41} can be seen for specimens (a) and (b) in Figure 3. Note that throughout the paper, "o"s and "x"s will denote curves regarding specimen (a) and specimen (b), respectively.

Figure 3 shows that R_{41} has a very similar trend for both specimens, with the curves altering with a maximum difference of 5 dB. The sound reduction index is quite high, with a R_w of 66 for both specimens.

4.2. $R_{4,situ}$, Floor-Ceiling Path In-situ

In order to obtain the transmission via the floor-ceiling path, $R_{4,situ}$, all of the walls need to be shielded. The direct sound insulation of the floor-ceiling assembly was measured only in the flanking sound transmission facility and not in the conventional lab, under the assumption that losses of the floor in the lab and in-situ are the same, both dominated by the high internal losses of the wood floor assembly itself. According to ISO 15712, edge losses can be ignored for wood framed construction.

Figure 4 shows that the direct sound reduction index through the floor of specimen (b), $R_4(b)$, is approximately 15 dB lower than that of the path of interest, R_{41}. Furthermore, the direct sound reduction index through the floor of specimen (a) is 15-20 dB lower than for specimen (b). The coincidence dip due to the gypsum board ceiling around 2 kHz is more pronounced for specimen (b), where the gypsum board is attached via resilient channels.

4.3. $R_{1,situ}$, Concrete Masonry Wall In-situ

In the flanking facility the in-situ sound reduction index of the wall was obtained through a series of shielding scenarios on the 4-room specimen. Between room C and D there are 4 paths across the ceiling wall junction (four unknowns); and therefore four shielding conditions are necessary to extract the path directly through the wall, as the ceiling cannot be shielded practically. The conditions are:

1. Shielding on both sides of the wall (measuring only ceiling-ceiling path)
2. Shielding only on one side of the wall (measuring ceiling-ceiling and wall-ceiling paths)
3. Shielding case 2) in reverse
4. And finally no shielding (measuring all four paths)

Using these four measurements (equations), all four paths can be resolved. The weighted sound reduction index for the wall is $R_w = 48$.

4.4. $\overline{D_{v,41}}$, Direction-Averaged Level Difference

The direction averaged junction level difference $\overline{D_{v,41}}$ was determined according to ISO 10848-1, by exciting the elements with a hammer for 30 seconds like rain on the roof. Three repeat measurements for each of the four excitation positions were made, and for each excitation the velocity on all elements was measured with four sensors on each at a time.

When measuring between elements 4 and 1, element 4 was excited on the top (the floor in room A) and measurements were made on the ceiling (room C) and on the wall (room C) as shown in blue in Figures 5 and 6. However, when measuring between 1

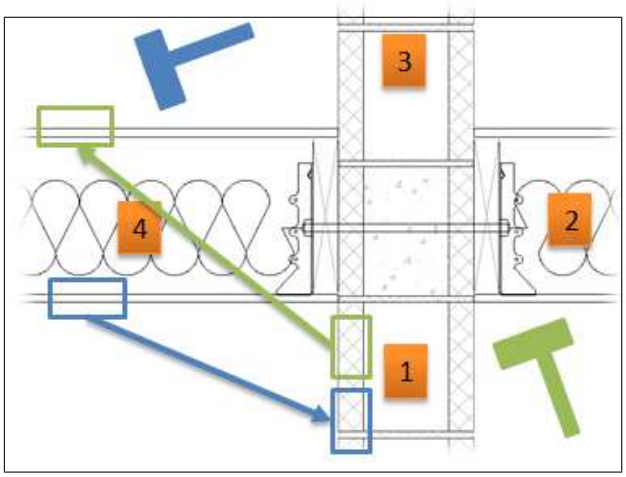

Figure 5. Excitation and measurement locations for determination of $D_{v,41}$ for "correct" approaches (1) were $D_{v,14}$ is represented in green and $D_{v,41}$ in blue.

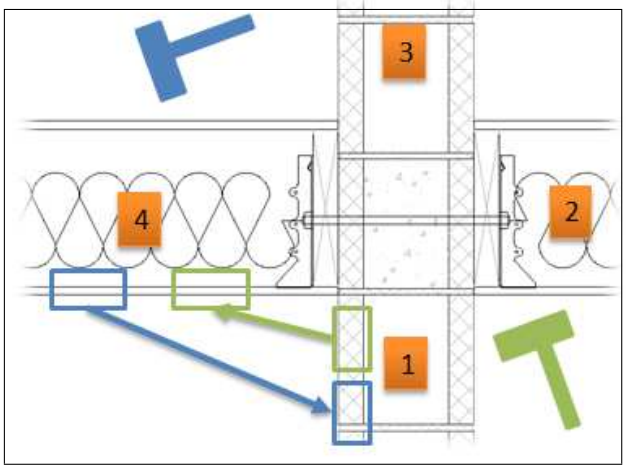

Figure 6. Excitation and measurement locations for determination of $D_{v,41}$ for "false" approaches (1) were $D_{v,14}$ is represented in green and $D_{v,41}$ in blue.

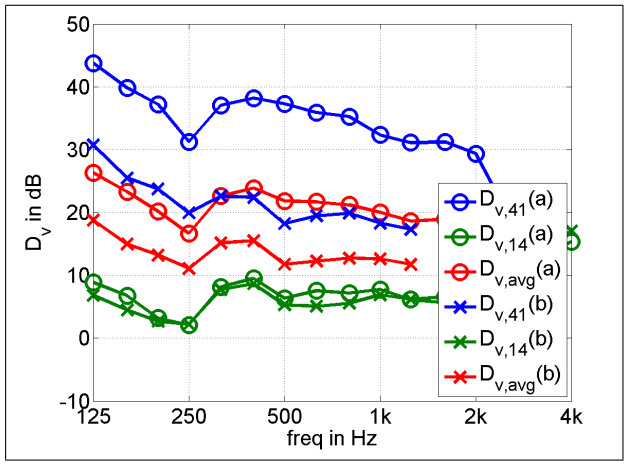

Figure 7. Measured "correct" velocity level difference between ceiling and wall $D_{v,41}$, wall and floor $D_{v,14}$, and average thereof ($\overline{D_{v,41}}$ or $D_{v,avg}$) for specimens (a)-o's and (b)-x's using approach (1).

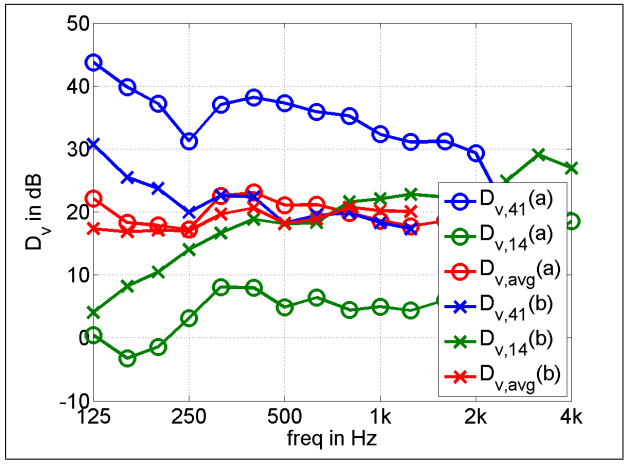

Figure 8. Measured "false" velocity level difference between ceiling and wall $D_{v,41}$, wall and ceiling $D_{v,14}$, and average thereof ($\overline{D_{v,41}}$ or $D_{v,avg}$) for specimens (a)-o's and (b)-x's using approach (2).

and 4, two different approaches were used. The first approach (1) was according to Schoenwald [8], where element 1 was excited in room C (side is not relevant for homogeneous elements) and measurements were made on the top of element 4 (floor in room A) as shown in Figuree 5. The second approach (2), just to capture an error often made in the field, element 1 was excited in room C and measurements were made on the bottom of element 4 (ceiling in room C) as common practice for heavy monolithic construction (see Figures 6), but not for lightweight construction. The results for are given for the "correct" approach (1) in Figure 7 and in Figure 8 for the "false" approach (2).

Note that the velocity level differences are not simply proportional to the energy in the elements because the masses are very different. For both approaches (1) and (2), the results from element 1 to 4 and from 4 to 1 are not reciprocal as described by Mahn in [7], as the wood joist floor cannot be seen as homogeneous element entertaining a diffuse wave field. The velocity level differences could not be measured accurately up to 4 kHz due to a low signal to noise ratio, especially for the path from element 4 to 1. The curves are discontinues where the signal to noise ratio exceeds 6 dB.

For the "correct" approach (1) shown in Figure 7, the velocity level difference for the wall-floor path D_{v14} is the same for both specimens. In other words, D_{v14} is independent of the ceiling details. The ceiling-wall path D_{v41} is as expected very dependent on the attachment of the ceiling, and approximately 10-15 dB greater for specimen (a) with directly attached ceiling than for specimen (b). This is because the velocity of the ceiling (b) is much lower than that of specimen (a). The averaged velocity level difference for specimen (a) is therefore also greater than for specimen (b), but only by approximately half (5-7 dB).

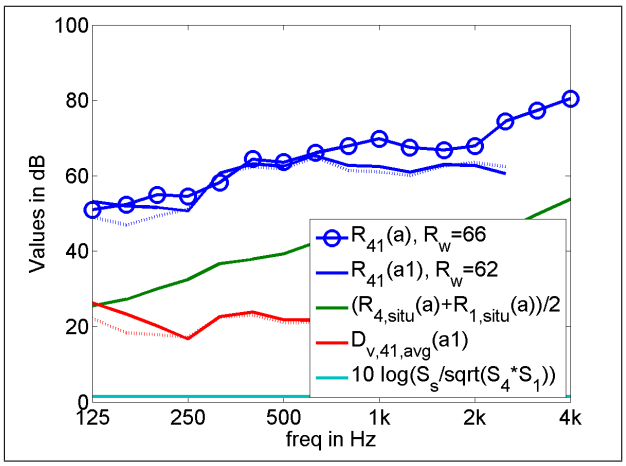

Figure 9. Measured and predicted flanking reduction index from floor to wall for specimen A, together with values used to calculate the predicted levels. Dashed lines are values calculated using "false" approach.

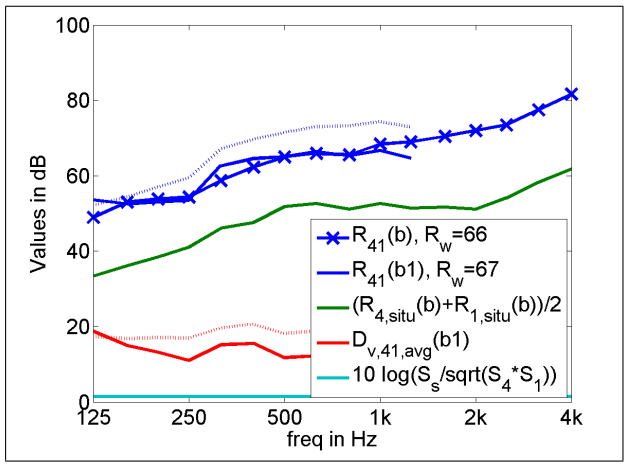

Figure 10. Measured and predicted flanking reduction index from floor to wall for specimen B, together with values used to calculate the predicted levels. Dashed lines are values calculated using "false" approach

For the "false" approach (2) shown in Figure 8, the velocity level differences for the wall-ceiling and ceiling-wall path are quite different for both specimens. However, the direction-averaged velocity level difference is very similar for both specimens.

4.5. Summary of Measured Results

In this section the measured results for all four cases (two specimens determined using two approaches for measuring $\overline{D_{v,41}}$) are presented. In Figure 9, the full measured R_{41} is plotted with all of the other components of Equation 2. The surface correction constant for all of the cases contributes the least to the overall flanking sound reduction index, followed by $\overline{D_{v,41}}$. As stated earlier, for the tests conducted in this study, the direction averaged velocity level difference $D_{v,41}$ is very similar measured using the two different approaches. The average of the two direct sound reduction indexes contributes the most to the R_{41} value. Both path estimates under-predict the full floor-wall path, shown by the three blue curves. The line with the circles was measured using the ISO 10848 indirect method, the solid one used the "correct" approach, and the dashed one used the "false" approach. As the top and bottom of element 4 have similar velocity levels, the approaches give very similar answers, but both under-predict the single number rating R_w by 4 points (62). It was possible to determine R_w accurately although $\overline{D_{v,41}}$ didn't continue with confidence to 3.15 kHz, because these single number ratings are controlled in the low frequency range.

For the second specimen (b) shown in Figure 10, the different approaches give different results. Using the "correct" approach only slightly over-predicts the performance, and the single number rating by only one point. However, using the "false" approach over-predicts R_w by 5 points leading to a value of 71.

5. Conclusion and Outlook

Although the path investigated here does not contribute significantly to the overall apparent sound reduction index from the upper room A to the lower room C, the investigation was helpful in understanding what influence the location of measuring the velocity level difference has on different types of construction. Where the gypsum board ceiling is directly attached, velocity level differences can be made using the "correct" or "false" approach, as the velocity on both sides of the element are comparable, similar to a homogeneous element. However, if the OSB subfloor and gypsum board ceiling were not directly attached to the joists, or if they did not have similar mass per areas, this "false" approach wouldn't work. Note that for assemblies with such low sound reduction indices, only the direct path needs to be characterized as the others can be neglected.

However,in the case of specimen (b), with the resilient channels, the location of the measurement is very important. This paper further confirms that the "correct" approach gives much better results, even for hybrid construction.

In the next steps other paths will be investigated, all with measured input parameters as well as estimated input parameters as suggested in the appendix of ISO 15712 and as already presented in the related impact sound transmission study [5].

Until all of the different scenarios and types of construction are evaluated for lightweight construction, it is believed that the indirect shielding method gives the most accurate results. However, it is also appreciated that this method is the most cumbersome to carry out, because a very sophisticated lab is required.

Acknowledgement

The authors would like to thank the Canadian Concrete Masonry Producers Association (CCMPA) for funding this research.

References

[1] International Organization for Standardization, ISO 15712, Building acoustics - Estimation of acoustic performance of buildings from the performance of elements, (2005).

[2] International Organization for Standardization, ISO 10140, Acoustics - Laboratory measurement of sound insulation of building elements, (2010).

[3] International Organization for Standardization, ISO 10848, Acoustics – Laboratory measurement of the flanking transmission of airborne and impact sound between adjoining rooms, (2006).

[4] T.R.T. Nightingale, J.D. Quirt, F. King and R.E. Halliwell, RR-218, Flanking Transmission in Multi-Family Dwellings Phase IV, (2006).

[5] B. Zeitler, S. Schoenwald, I. Sabourin, Flanking sound insulation of wood frame assemblies with high axial and lateral load bearing capacity; Inter-Noise 2013, Innsbruck, Austria, Sept (2013).

[6] S. Schoenwald; T. Nightingale, B. Zeitler, F. King, Approaches for estimating flanking transmission for heavy impact sources, Inter-Noise 2010, Lisbon, Portugal, June (2010)

[7] Jeffrey Mahn, Prediction of Flanking Noise Transmission in Lightweight Building Constructions: A Theoretical and Experimental Evaluation of the Application of EN12354-1, PhD Thesis, Uniersity of Canterbury, (2009)

[8] S. Schoenwald, Comparison of proposed methods to include lightweight framed structures in EN 12354 prediction model, Euronoise 2012, Prag, Czech Republic, June (2012)

[9] ISO 10140: Acoustics – Laboratory Measurement of Sound Insulation of Building Elements – Part 2: Measurement of Airborne Sound Insulation. 2010.

[10] ISO 717: Acoustics – Rating of Sound Insulation in Buildings and of Building Elements – Part 1: Airborne Sound Insulation. 2013.